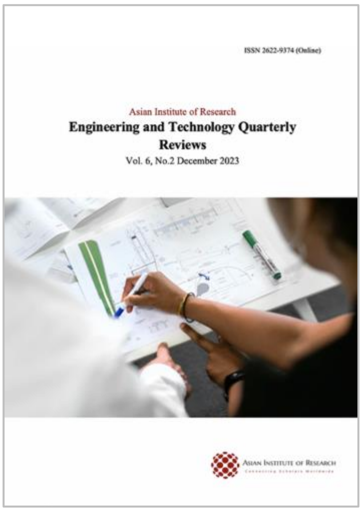

Engineering and Technology Quarterly Reviews

Kaplan, M. (2023), Computational Investigation on Flow and Power Output of Solar Chimney Power Plants by Changing Collector Entrance Geometry. In: *Engineering and Technology Quarterly Reviews*, Vol.6, No.2, 39-48.

ISSN 2622-9374

The online version of this article can be found at:
https://www.asianinstituteofresearch.org/

The Asian Institute of Research
Engineering and Technology Quarterly Reviews
Vol.6, No.2, 2023: 39-48
ISSN 2622-9374

Computational Investigation on Flow and Power Output of Solar Chimney Power Plants by Changing Collector Entrance Geometry

Mahmut Kaplan[1]

[1] Department of Machine and Metal Technology, Naci Topcuoglu Vocational High School, Gaziantep University, Gaziantep, Turkey

Correspondence: Mahmut Kaplan, Department of Machine and Metal Technology, Naci Topcuoglu Vocational High School, Gaziantep University, Gaziantep 27600, Turkey. Tel: +90 536 231 92 81. E-mail: mahmutkaplan@gantep.edu.tr. ORCID: 0000-0003-2675-9229.

Abstract
The use of fossil fuels for generating power has leaded to the reduction of fossil fuel resources and many adverse influences involving climate change and environmental pollution. Solar energy has a potential to provide eco-friendly energy with a great energy supply for producing heat and electricity. Basic parts of the system are the collector, chimney and turbine. The collector is a vital component of the system and its geometrical features noticeably influence the power plant efficiency. In the current work, a three dimensional computational fluid dynamics (CFD) simulation of a SCPP based on the Manzanares prototype is performed to scrutinize the impact of collector entrance height (H_e) ranging from 0.75 m to 2 m on the solar chimney power output. Computational model is developed by employing RNG k-ε turbulence and discrete ordinates (DO) coupled with solar ray tracing models through ANSYS Fluent software. The model is validated using measured data published in the literature. The numerical results reveal that reducing He improves maximum velocity (V_{max}), power output and pressure difference in the turbine at the expense of decreasing air mass flow rate. The highest velocity of 19.45 m/s is achieved with H_e = 0.75 m and V_{max} enhances by 36.20% compared to base model with H_e = 1.85 m at 1000 W/m^2. Besides this configuration provides the maximum power output of 66.51 kW and augments power output to 31.74% compared to the base case at 1000 W/m^2.

Keywords: Solar Chimney, CFD, Collector Entrance Height, Maximum Velocity, Pressure Drop, Power Output

1. Introduction

Renewable energy is energy generated from abundant and continuously replenished natural resources including solar, wind, hydro, tidal, geothermal, biomass and wastes. It is a key to reduce the dependence on fossil fuels and thus to have a safer, cleaner, and sustainable world (Peake, 2018). Solar energy has a potentially critical role in

providing eco-friendly energy for generating electricity and heat (Tyagi et al., 2020). The solar chimney system is capable of producing the electric power from the solar energy with no greenhouse gases emission, especially in rural areas where solar chimney power plant (SCPP) technology offers freely available energy resources to augment access to electrical energy (Okoye & Taylan, 2017). SCPP is established on three technologies (the greenhouse, chimney and wind turbine) joined together to harness energy from the sun (Kasaeian et al., 2017).
Major components of a solar chimney are chimney, collector and turbine. The collector whose roof made up of a semi-transparent material (plastic or glass) received the solar radiation into the system and then transmitted to the ground which leads to a rise in temperature here. Namely, the greenhouse effect is generated by the semi-transparent collector surface through which the short wavelengths of visible light from the sun pass but the longer wavelengths of the solar radiation are unable to pass. This elevates the ground temperature under the collector. Thus, the heat transfer takes places between the heated ground surface and fresh air coming from the collector entrance. Temperature difference on the ground results in density gradient which produces a buoyancy force. Therefore the heated system air moves upwards and it is directed towards the outlet of the chimney. With a long tubular geometry, the chimney generates a pressure difference and augments the velocity of the system air. SCPP uses the buoyancy-induced convective flow which rotates the turbine installed close to the inlet of the chimney. The turbine converts the air kinetic energy to the rotational energy and eventually into electricity in a generator (Pradhan et al., 2021).

Heat is stored in the natural soil but an additional absorber (energy storage) layer under the roof is needed to meet the requirement of SCPP system working during the night or cloudy days (Guoa et al., 2019). The absorber stores the thermal energy transferred by the collector and employs it to heat air during the absence of sun providing electricity production for 24 hours. The selection of a suitable absorber material is crucial to improve operational performance of the SCPP system. Aluminium, canvas, black and clear visqueen are used as absorber plate materials (Das & Parvathy, 2022). Besides, thermal storage capacity of SCPP is improved by introducing water filled black tubes laid on the ground to store heat during day. At night-time, the water in the tubes emits the heat while the air inside the collector beginning to cool (Zhou et al., 2010).

Geometrical parameters of solar chimney components such as collector and chimney influence performance of SCPP systems (Cuce et al., 2022). Main geometric features of the system are the collector height, radius and slope and the chimney diameter and height. Besides divergent and convergent collector and chimney design impacts the efficiency of SCPP system.

Researchers recently examined different collector geometries to enhance performance of SCPP systems. Hassan et al. (2018) accomplished computational research on changing the slope of the collector (4°-10°) and chimney divergent angle (1°-3°) with fixed other geometric parameters to intensify the system performance employing ANSY Fluent CFD codes. They pointed out that the chimney having 1° divergent angle leaded to remarkable increment in maximum airflow velocity and power output at smaller chimney height. Golzardi et al. (2021) conducted the experimental tests and a three dimensional (3D) CFD analysis to scrutinize the influences of collector entrance of square and circular collectors on airflow velocity and heat transfer characteristics inside the chimney. They observed that reducing collector entrance of square collector by one-half and that of circular collector by one-quarter augmented outlet velocity and thermal efficiency of the chimney. Cuce (2022) introduced a 3D model based on Manzanares pilot plant to explore the effect of the dimensionless parameter called collector radius rate (collector radius/ the pilot plant collector radius) on power output for the 90° model by ANSYS Fluent. Their results displayed that a rise in the collector radius rate enhanced power generated by the plant but at a certain collector size (upto one and a half times the collector radius) and then the efficiency diminished due to the high cost and an increase in the space occupied by the collector.

According to the available literature review, the collector geometric characteristics significantly influence air flow and power production in the system. In the current work, new collector geometries are developed by varying the height of the collector entrance (H_e) from 0.75 m to 2 m for fixed collector length and chimney geometric parameters. The distance between the ground level and chimney inlet is also kept constant. Since the region between chimney inlet and collector outlet is altered by changing He for each configuration, the introduced solar chimney geometries in this work are different from previous CFD investigations [Cuce et al., 2022a; Hassan et al., 2018; Golzardi et al., 2021; Cuce, 2022; Sen et al., 2021). The impacts of new produced configurations on the solar chimney performance characteristics are analyzed and discussed by considering material and environmental features of the Manzanares pilot facility using ANSYS Fluent.

2. Materials and methods

In the present work, governing equations (continuity, momentum and energy) combined with the discrete ordinates (DO) radiation and turbulence models are solved in a coupled manner via ANSYS Fluent. Discrete ordinate (DO) radiation model is employed to stimulate solar rays passing through the semi-transparent (glass) collector. Ray tracing option in solar load model is selected to include impacts of incident solar radiation from the sun's rays in the calculation. Assume that the flow in the SCPP system is turbulent, incompressible, 3D and steady-state. Since the RNG k-ε turbulence model simulates the flow within the system well (Hassan et al., 2018; Cuce, 2022; Sen et al., 2021; Hachicha et al., 2023), this model is utilized in this study. The kinetic energy (k) and dissipation rate (ε) equations in the model are (ANSYS Fluent, 2018):

$$\frac{\partial}{\partial x_i}(k\rho u_i)+\frac{\partial}{\partial t}(k\rho)=\frac{\partial}{\partial x_j}\left(\mu_{eff}\alpha_k\frac{\partial k}{\partial x_j}\right)+G_k+G_b-\rho\varepsilon-Y_M+S_k \quad (1)$$

$$\frac{\partial}{\partial x_i}(\varepsilon\rho u_i)+\frac{\partial}{\partial t}(\varepsilon\rho)=\frac{\partial}{\partial x_j}\left(\mu_{eff}\alpha_\varepsilon\frac{\partial \varepsilon}{\partial x_j}\right)+C_{1\varepsilon}\frac{\varepsilon}{k}\left(C_{3\varepsilon}G_b+G_k\right)-C_{2\varepsilon}\rho\frac{\varepsilon^2}{k}-R_\varepsilon+S_\varepsilon \quad (2)$$

The Boussinesq approximation is applied to determine air density change in the system as appropriate for modeling the buoyancy flow.

$$(\rho-\rho_a)g\approx-\rho_a\beta(T-T_a) \quad (3)$$

where ρ_a and T_a are air density and temperature. β and g present the thermal expansion coefficient and gravitational acceleration.
Power output, P_o of the SCPP system is determined by:

$$P_o=\eta_t Q_v \Delta P_t \quad (4)$$

where η_t is the efficiency of turbine which is generally taken to be 0.8 (Abdelmohimen & Algarni, 2018; Cuce et al., 2020; Mebarki et al., 2022). Q_v is the volume flow rate of air. ΔP_t is pressure drop in the turbine. It is determined by calculating the average pressure difference (P_t) at the turbine considered to be located 9 m above ground level using the CFD simulation (Cuce et al., 2020).

$$\Delta P_t=r_t P_t \quad (5)$$

where r_t is the turbine pressure drop ratio and $r_t = 2/3$ (Mebarki et al., 2022).
The 3D geometric model is built in the ANSYS DesignModeler. The geometric features of the developed model are determined with reference to the Manzanares solar chimney constructed dimensions in Table 1 (Haaf et al., 1983).

Table 1: Model dimensions based on the Spanish prototype

Geometric characteristics	**Value**
The radius and height of the collector	122 m - 1.85 m
The radius and height of the chimney	5.08 m - 194.6 m
The thickness of the ground	0.5 m

The thicknesses of chimney and collector are 0.00125 m and 0.004 m. As illustrated in Figure 1(a), instead of simulating the full geometry, 15° CFD model of Manzanares prototype is improved to reduce the computational time. The model geometry is meshed with an unstructured tetrahedral grid using ANSYS Meshing as demonstrated in Figure 1(b).

The boundary conditions adapted to CFD model are illustrated in Fig. 1(a). Pressure inlet and outlet boundary conditions are applied at the collector inlet and the chimney outlet respectively. The atmospheric pressure is specified at the inlet and outlet. Wall boundary conditions are assigned to surfaces of the ground, collector and chimney as demonstrated in Figure 1(a). The opaque and adiabatic wall boundary conditions are defined at the ground and chimney walls, respectively. Convection thermal boundary condition is employed for the collector and heat transfer coefficient is fixed to 10 W/m^2K [20]. The collector is considered as semi-transparent. Ambient air temperature and density is 293.15 K and 1.2046 kg/m^3. To reduce computational domain, symmetry boundary condition is applied on two symmetric planes as shown in Figure 1(a).

In order to setup CFD simulation, the component's thermophysical properties in Table 2 are defined in ANSYS Fluent. The equations are discretized using the finite volume approach. SIMPLE scheme is used for pressure-velocity coupling. The pressure is interpolated using a PRESTO method while momentum, turbulence and energy terms were spatially discretized using the second-order upwind scheme.

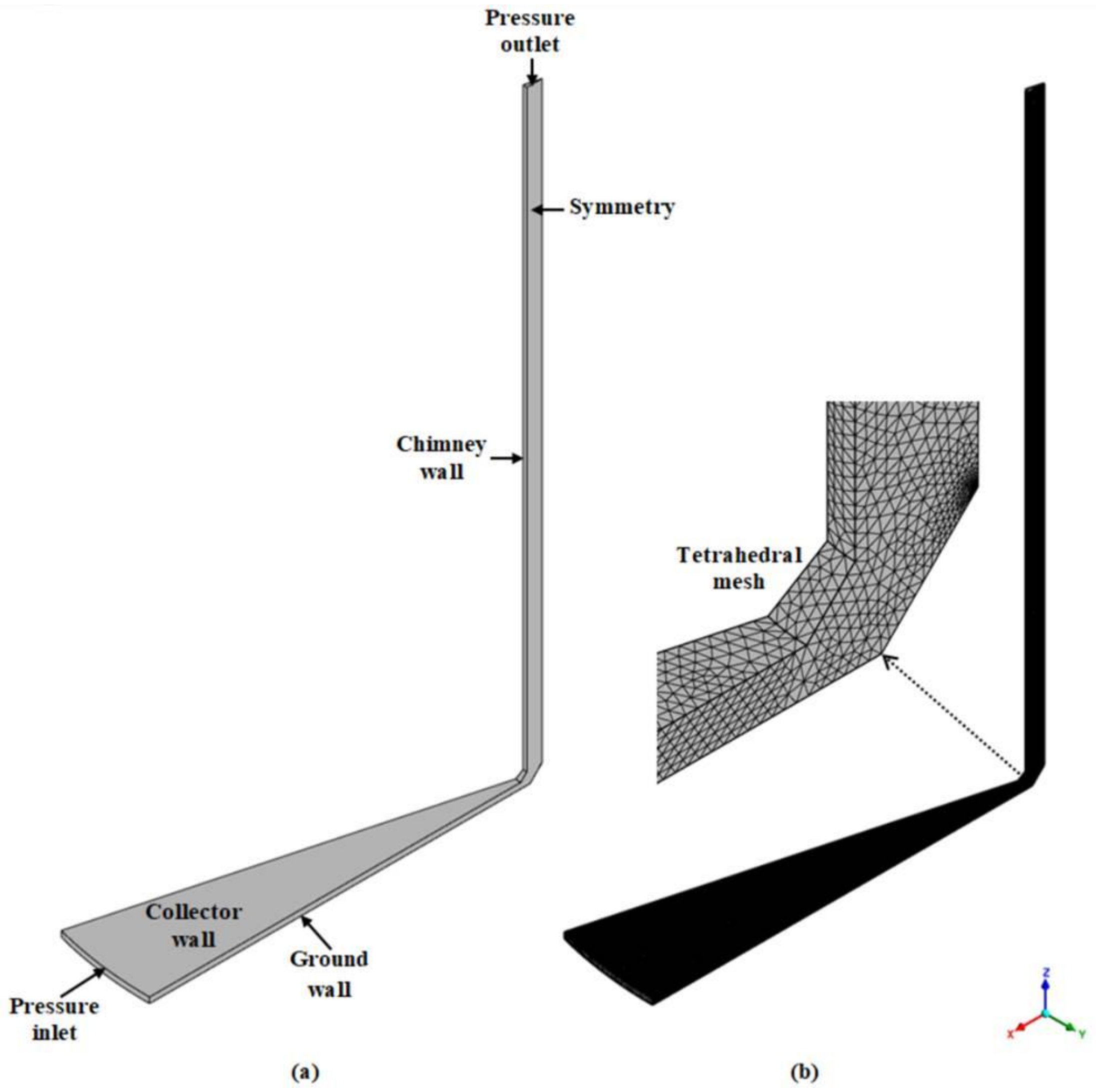

Figure 1: (a) Computational model and boundary conditions, (b) grid structure of the model

Table 2: Thermophysical features of the components employed in CFD simulation

Properties	Chimney	Collector	Ground
Thermal conductivity (W/mK)	202.4	1.15	1.83
Density (kg/m^3)	2719	2500	2160
Specific heat (J/kgK)	871	750	710

3. Results and discussions

In the current study, the impact of distinct collector entrance configurations on fluid flow and performance characteristics is analyzed employing ANSYS Fluent based on finite volume method. Prior to carrying out CFD simulation, the grid-independent study is conducted for three different mesh sizes. V_{max} values of three grid configurations are demonstrated in Table 3. For mesh number of 386041, percentage variation in V_{max} is examined to be 0.92 at 1000 W/m^2. Comparison of similar studies from literature indicates that this variation is well suited for the simulation and thus this element size is chosen for the rest of the research.

Table 3: The results of grid independent test for CFD model

Number of cell	V_{max} (m/s)	% change in V_{max}
192746	13.63	-
268921	14.15	3.82
348018	14.28	0.92

The model is verified with the measured data of the Manzanares's chimney (Rabehi et al., 2017) and compared with previous numerical studies in Figure 2.

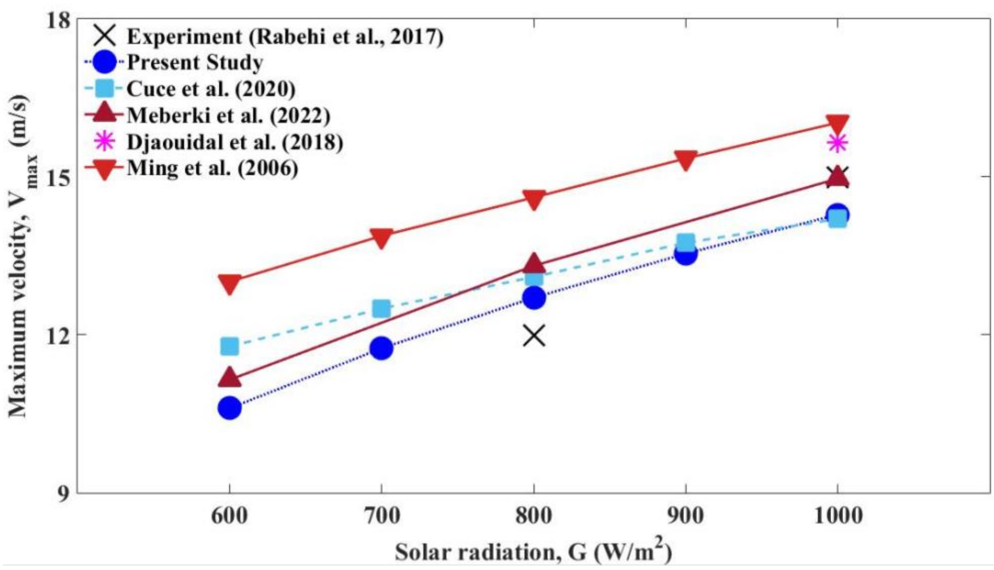

Figure 2: Comparison of maximum velocity values of the base CFD model with calculated and measured data available in literature

In comparison to results from previous studies, computed maximum velocity values are in good agreement with the measured values at 800 and 1000 W/m^2. Besides, it is consistent with Cuce et al.'s (2020) and Meberki et al.'s (2022) numerical studies at 600-1000 W/m^2.

Figure 3 demonstrates the variation of V_{max} as a function of H_e ranging 0.75 m to 2 m at 800 and 1000 W/m^2.

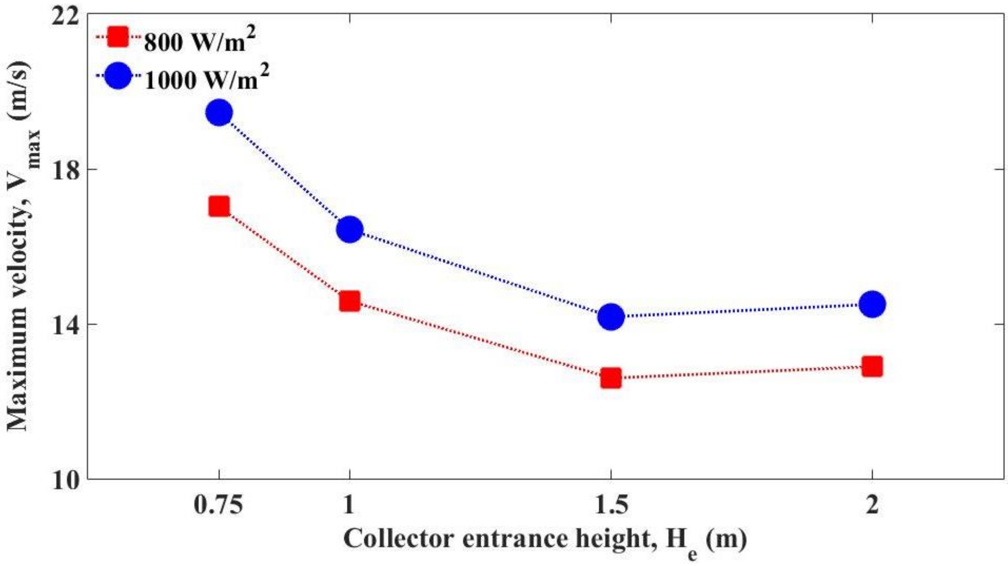

Figure 3: Variation of maximum velocity with collector entrance height

It is obvious from Figure 3 that there is a nonlinear relationship between V_{max} and H_e. A slight decrease in Vmax is observed from H_e = 2 m till H_e = 1.5 m and then V_{max} is significantly enhanced with decreasing H_e. The highest air velocity of 19.45 m/s is obtained for H_e = 0.75 m compared the base model having V_{max} = 14.28 m/s at 1000 W/m^2. The reason behind this sharp increase is that the collector inlet area is reduced significantly with H_e = 0.75 m and this leads to notable enhancement in air velocity of the system.

In Figure 4, the regions near the turbine located and collector outlet are examined in detail to understand the impact of H_e on the distribution of air velocity at 1000 W/m^2.

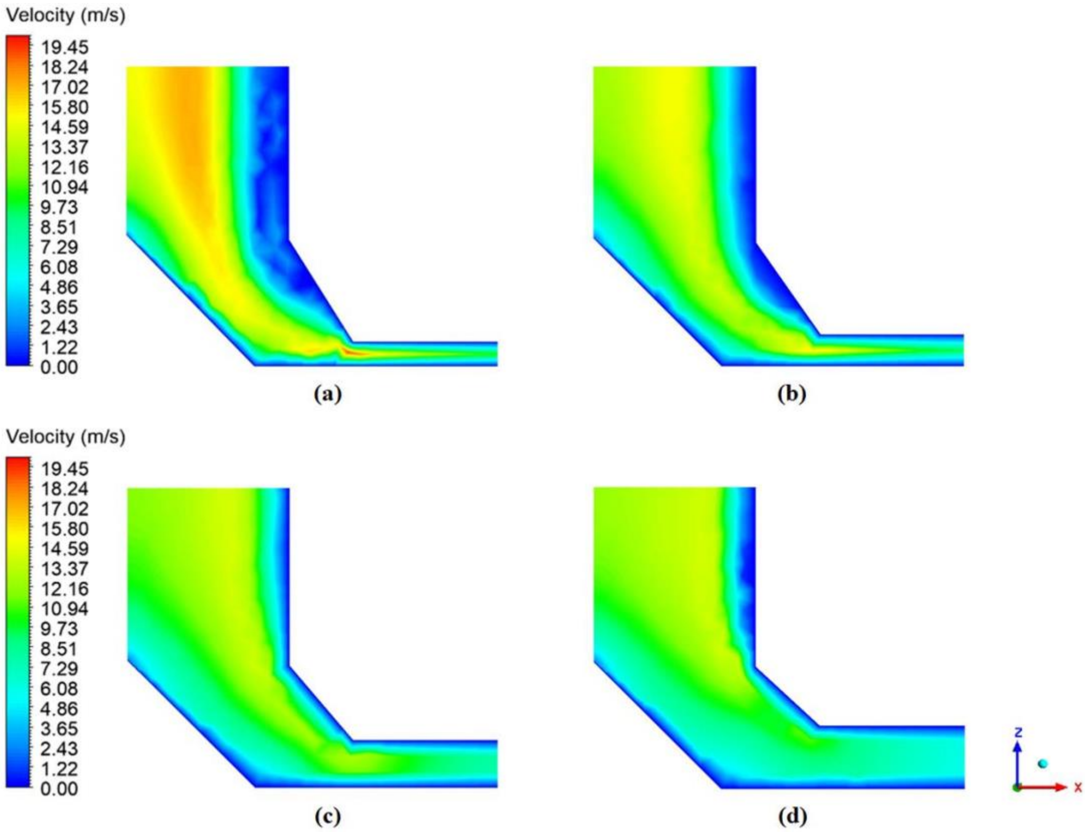

Figure 4: Air velocity distribution near the turbine installed and collector outlet for (a) H_e = 0.75 m, (b) H_e = 1 m, (c) H_e = 1.5 m and (d) H_e = 2 m at 1000 W/m^2

As illustrated in Figure 4, the area between the chimney inlet and collector outlet is varied with reducing He owing to the distance between the ground and chimney entrance remaining same. This leads to the enhancement of velocity distribution around the collector outlet and chimney inlet. Although maximum air velocity is diminished slightly for reducing H_e from 2 m to 1.5 m in Figure 3, the local air velocity around the collector outlet is augmented significantly with this configuration in Figure 4 (c). It is confirmed the aforesaid result that the configuration with H_e = 0.75 m intensifies air velocity remarkably in the region where turbine placed. It is important owing to the increased kinetic energy of the system improving electricity production from the chimney.

Air mass flow rate ($\dot{m}$) and pressure drop around turbine are two important parameters that impact the solar chimney efficiency. That is, P_o is strongly dependent the air volume flow rate and pressure difference across the turbine as seen in Equation 4.

Figure 5 demonstrates the variation of $\dot{m}$ as a function of H_e ranging 0.75 m to 2 m at 800 and 1000 W/m^2. As illustrated in Figure 5, a decreasing trend of $\dot{m}$ is observed with a decrease in H_e. It is expected that $\dot{m}$ values for H_e = 0.75 and 1 m should be elevated because of these configurations notably enhancing V_{max} in Figure 3. But the collector entrance area is decreased with reducing H_e and this causes lower air mass flow rate within the chimney. $\dot{m}$ is 728 kg/s for H_e = 0.75 m compared to the base case with $\dot{m}$ = 1062 kg/s.

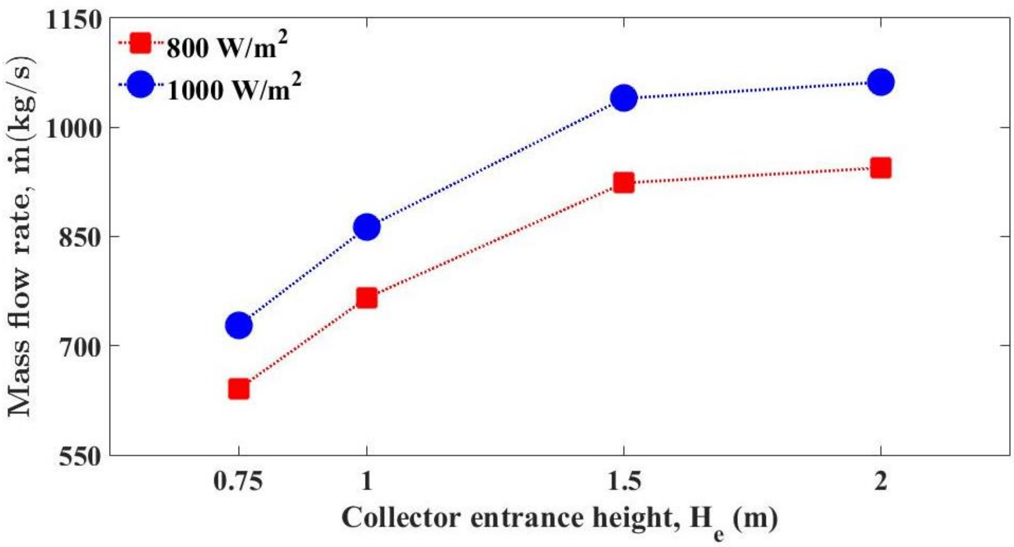

Figure 5: Variation of mass flow rate with collector entrance height

Figure 6 shows the change of pressure difference in a turbine as a function of H_e ranging 0.75 m to 2 m at 800 and 1000 W/m^2. As seen in Figure 6, the lower collector entrance results in a larger pressure drop through the turbine. The highest pressure drop of 206.3 Pa is achieved for He = 0.75 m at 100 W/m^2.

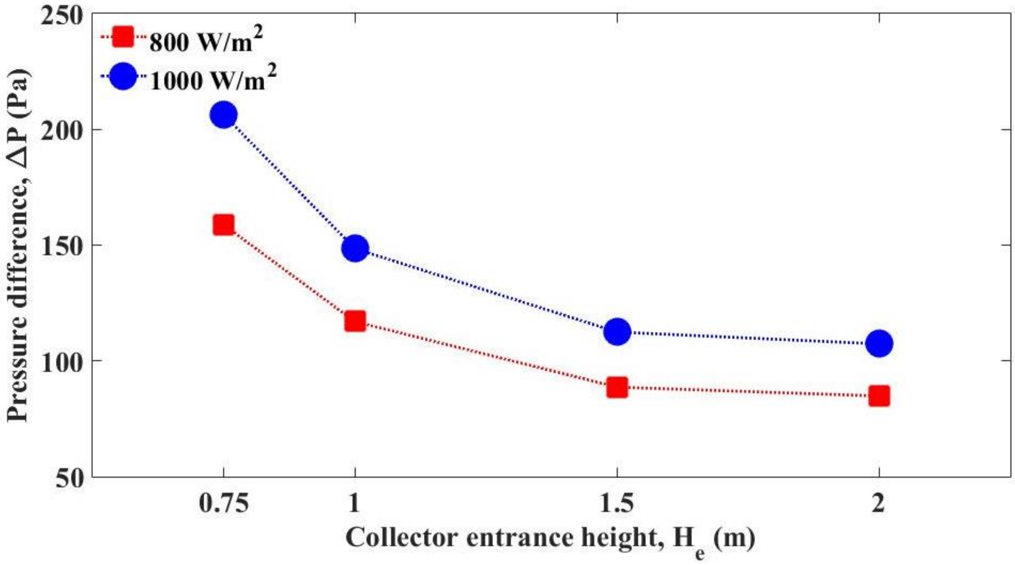

Figure 6: Variation of pressure drop in a turbine with collector entrance height

Figure 7 demonstrates the change of P_o of the SCPP system as a function of H_e ranging 0.75 m to 2 m at 800 and 1000 W/m^2. As shown in Figure 7, a reduction in H_e yields to enhancement in P_o of the system at both 800 and 1000 W/m^2.

It is noticed that pressure difference where the turbine placed plays a dominant role in augmenting P_o of the solar chimney. Namely, the increased pressure drop with narrow collector entrance in Figure 6 leads to a significantly rise in P_o of the chimney, especially at 1000 W/m2. It is concluded that decreasing air mass flow rate with a lower collector entrance is compensated by higher pressure drop gained near the turbine. Therefore for H_e = 0.75, the maximum P_o of 66.51 kW is achieved and this configuration improves P_o to 31.74% in comparison to the base model at 1000 W/m^2.

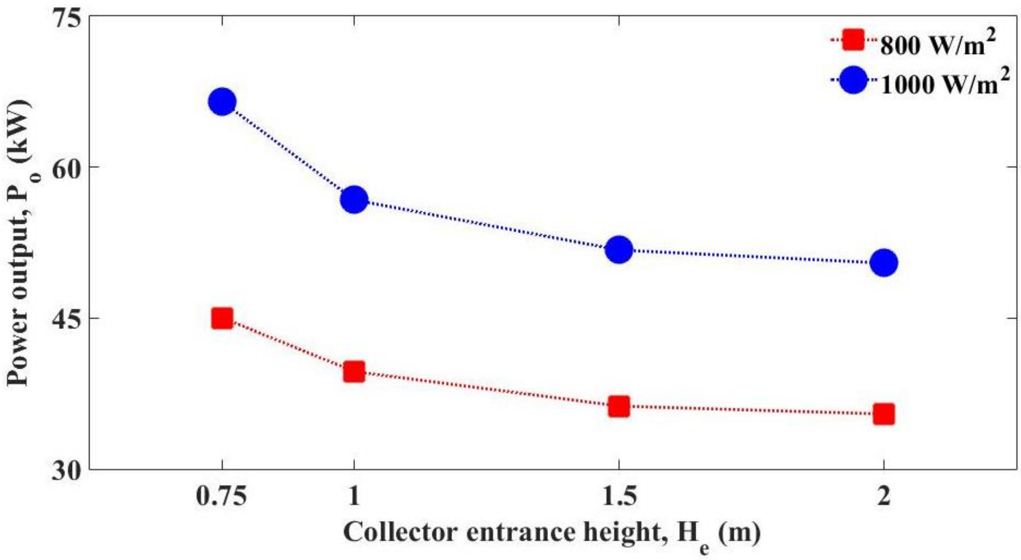

Figure 7: Variation of power output of the system with collector entrance height

4. Conclusions

This paper examines numerically the impact of the entrance height of the collector on enhancement of power production in a solar chimney system by constructing a 3D model employing ANSYS Fluent CFD code based upon the finite volume discretization. The collector height is changed from 0.75 m to 2 m by other dimensions of the components and the distance between the ground and chimney entrance of the model keeping unchanged.

After grid independent test and verification of the model, performance characteristics are evaluated as a function of H_e. The main findings are summarized as follows:

- The predicted V_{max} values obtained with the present CFD model agree well with measured data compared to the results of the former numerical studies at 800 and 1000 W/m^2.
- He is an influential geometric parameter that affects P_o of the system.
- New proposed configurations obtained by altering collector entrance with a constant distance between the ground and chimney inlet is more efficient to improve P_o of the plant for H_e = 0.75 and 1 m.
- Reducing air mass flow rate with decreasing He is met with higher pressure drop gained close to the turbine.
- The configuration with H_e = 0.75 m provides the highest P_o of 66.51 kW, V_{max} of 19.54 m/s and the maximum pressure drop of 206.3 Pa whereas this configuration reduces air mass flow rate by 31.39% compared to the base case at 1000 W/m^2.
- This study which provides key insights for determining appropriate collector entrance geometry to enhance the system's power output will be helpful for further solar chimney numerical analysis and designs.

Author Contributions: All authors contributed to this research.

Funding: Not applicable.

Conflict of Interest: The authors declare no conflict of interest.

Informed Consent Statement/Ethics Approval: Not applicable.

References

Abdelmohimen M. A. H., & Algarni S. A. (2018). Numerical investigation of solar chimney power plants performance for Saudi Arabia weather conditions. *Sustainable Cities and Society*, 38, 1–8. https://doi.org/10.1016/j.scs.2017.12.013

ANSYS FLUENT, *Theory Guide, Release 19.2*, ANSYS Inc., 2018.

Cuce E., Sen H., & Cuce P. M. (2020). Numerical performance modelling of solar chimney power plants: Influence of chimney height for a pilot plant in Manzanares, Spain. *Sustainable Energy Technologies and Assessments*, 39, 100704. https://doi.org/10.1016/j.seta.2020.100704

Cuce E., Saxena A., Cuce P. M., Sen H., Guo S., & Sudhakar K. (2021). Performance assessment of solar chimney power plants with the impacts of divergent and convergent chimney geometry. *International Journal of Low-Carbon Technologies*, 16(3),704–714. https://doi.org/10.1093/ijlct/ctaa097

Cuce E. (2022). Dependence of electrical power output on collector size in Manzanares solar chimney power plant: an investigation for thermodynamic limits. *International Journal of Low-Carbon Technologies*, 17, 1223–1231. https://doi.org/10.1093/ijlct/ctac094

Cuce E., Cuce P. M., Carlucci S., Sen H., Sudhakar K., Hasanuzzaman M., & Daneshazarian R. (2022). Solar chimney power plants: a review of the concepts, designs and performances. *Sustainability*, 14(3), 1450. https://doi.org/10.3390/su14031450

Das P., & Parvathy C. V. (2022). A critical review on solar chimney power plant technology: influence of environment and geometrical parameters, barriers for commercialization, opportunities, and carbon emission mitigation. *Environmental Science and Pollution Research*, 29, 69367–69387. https://doi.org/10.1007/s11356-022-22623-7

Djaouida B., Aouachria Z., Benmachiche A. H, & Ali S. (2020). Controlling power output of solar chimney power plant according to demand. *International Journal of Ambient Energy*, 41(13), 1467–1481. https://doi.org/10.1080/01430750.2018.1517677

Golzardi S., Mehdipour R., & Baniamerian Z. (2021). How collector entrance influences the solar chimney performance: experimental assessment. *Journal of Thermal Analysis and Calorimetry*, 146, 813–826. https://doi.org/10.1007/s10973-020-10031-3

Guoa P., Lia T., Xub B., Xuc X., & Lia J. (2019). Questions and current understanding about solar chimney power plant: a review. *Energy Conversion and Management*, 182, 21–33. https://doi.org/10.1016/j.enconman.2018.12.063

Haaf W., Friedrich K., Mayr G., & Schlaich J. (1983). Solar chimneys part I: principle and construction of the pilot plant in Manzanares. *International Journal of Solar Energy*, 2, 3–20. https://doi.org/10.1080/01425918308909911

Hachicha A. A., Abo-Zahhad E. M., Oh S., Issa S., & Rahman S. M. A. (2023). Numerical investigation and optimization of a novel hybrid solar chimney for air pollution mitigation and clean electricity generation. *Applied Thermal Engineering*, 226, 120271. https://doi.org/10.1016/j.applthermaleng.2023.120271

Hassan A., Ali M., & Waqas Ali. (2018). Numerical investigation on performance of solar chimney power plant by varying collector slope and chimney diverging angle. *Energy*, 142, 411–425. https://doi.org/10.1016/j.energy.2017.10.047

Kasaeian A. B., Molana S., Rahmani K., & Wen B. (2017). A review on solar chimney systems. *Renewable and Sustainable Energy Reviews*, 67, 954–987. https://doi.org/10.1016/j.rser.2016.09.081

Mebarki A., Sekhri A., Assassi A., Hanafi A., & Marir B. (2022). CFD analysis of solar chimney power plant: finding a relationship between model minimization and its performance for use in urban areas. *Energy Reports*, 8, 500–513. https://doi.org/10.1016/j.egyr.2021.12.008

Ming T., Liu W., & Xu G. (2006). Analytical and numerical investigation of the solar chimney power plant systems. *International Journal of Energy Research*, 30, 861–873. https://doi.org/10.1002/er.1191

Okoye C. O., & Taylan O. (2017). Performance analysis of a solar chimney power plant for rural areas in Nigeria. *Renewable Energy*, 104, 96–108. https://doi.org/10.1016/j.renene.2016.12.004

Peake S. (2018). *Renewable energy: power for a sustainable future*. Oxford University Press.

Pradhan S., Chakraborty R., Mandal D. K., Barman A., & Bose P. (2021). Design and performance analysis of solar chimney power plant (SCPP): a review. *Sustainable Energy Technologies and Assessments*, 47, 101411. https://doi.org/10.1016/j.seta.2021.101411

Sen H., Cuce P. M., & Cuce E. (2021). Impacts of collector radius and height on performance parameters of solar chimney power plants: a case study for Manzanares, Spain. *Recep Tayyip Erdogan University Journal of Science and Engineering*, 2(2), 83–104. https://doi.org/10.53501/rteufemud.1017909

Rabehi R., Chaker A., Aouachria Z., & Ming T. (2017). CFD analysis on the performance of a solar chimney power plant system: case study in Algeria. *International Journal of Green Energy*, 14(12), 971–982. https://doi.org/10.1080/15435075.2017.1339043

Tyagi H., Chakraborty P. R., Powar S., & Agarwal A. K. (2020). *Solar Energy Systems, Challenges, and Opportunities*, Springer.

Zhou X., Wanga F., & Ochieng R. M. (2017). A review of solar chimney power technology. *Renewable and Sustainable Energy Reviews*, 14(8), 2315–2338. https://doi.org/10.1016/j.rser.2010.04.018